Assessing Burn Severity and Vegetation Impact Using Sentinel-2 Satellite Imagery and Geospatial Analysis in Mae Ka Subdistrict, Mueang District, Phayao, Thailand

Anucharn, T.,[1] Sriprom, T.,[2] Chaikaew, N.[2] and Iamchuen, N. [2*]
[1]Information Technology, School of Information and Communication Technology, University of Phayao, Phayao, Thailand, E-mail: niti.ia@up.ac.th*
[2]Geographic Information Science, School of Information and Communication Technology, University of Phayao, Phayao, Thailand
**Corresponding Author*

DOI: https://doi.org/10.52939/ijg.v21i4.4067

Abstract
Wildfires are natural disasters that severely impact ecosystems, economies, and societies. Rapid and accurate detection and assessment of wildfire-affected areas are crucial for effective management and restoration. This research utilizes Sentinel-2 satellite imagery to investigate wildfire damage by analyzing pre- and post-fire satellite data to 1) analyze vegetation index changes before and after burning; 2) generate burn severity maps of the affected areas in Mae Ka subdistrict, Mueang district, Phayao, Thailand; and 3) examine the relationship between vegetation indices and burn severity levels. The study employs various spectral indices, including Normalized Burn Ratio (NBR), delta Normalized Burn Ratio (dNBR), Normalized Difference Water Index (NDWI), Relative Burn Ratio (RBR), and Normalized Difference Vegetation Index (NDVI). Results indicate that the monthly RBR index demonstrates high efficiency in detecting burned areas, with an overall accuracy of 90.6% and a Kappa coefficient of 0.76. Furthermore, the delta Normalized Difference Vegetation Index (dNDVI) effectively assesses wildfire impacts on vegetation. Areas experiencing severe burn impacts exhibit low dNDVI values, indicating significant vegetation damage. This study highlights the efficacy of satellite imagery and various spectral indices in evaluating wildfire damage. The Relativized Burn Ratio (RBR) performs better in burned area detection, while the dNDVI provides valuable insights into vegetation damage assessment. In conclusion, this research highlights the significant potential of integrating Sentinel-2 imagery with spectral indices in forest management. The methodology presented here offers a powerful tool for enhancing our capacity to assess, monitor, and respond to wildfire impacts, ultimately contributing to an effective and sustainable forest ecosystem management practices.

Keywords: Burned Area, Normalized Burn Ratio (NBR), Relativized Burn Ratio (RBR), Normalized Difference Vegetation Index (NDVI), delta Normalized Difference Vegetation Index (dNDVI), Visible Infrared Imaging Radiometer Suite (VIIRS)

1. Introduction

Wildfires are natural disasters that severely impact ecosystems, economies, and societies worldwide, particularly in regions with hot and dry climates such as Thailand. In recent years, Thailand has faced increasingly severe wildfire problems due to climate change and human activities. Global climate change has resulted in Thailand experiencing more erratic weather conditions, with continuously rising average temperatures leading to prolonged droughts and shorter rainy seasons, resulting in decreased rainfall [1]. These dry and extremely hot weather conditions act as catalysts for wildfires, especially in forested areas with high fuel accumulation, such as branches, leaves, and various organic materials [2] and [3]. Furthermore, the El Niño phenomenon, which increases sea surface temperatures in the tropical Pacific Ocean, is another factor contributing to severe droughts and increased wildfire risk in Thailand [4]. Human activities such as land clearing, agricultural burning, and improper fire management practices exacerbate these conditions, further elevating the risk of wildfires [5]. The socioeconomic impact of these wildfires is substantial, affecting agriculture, tourism, and local communities, with increased health risks from smoke and pollution [6].

Mae Ka Subdistrict, Phayao, Thailand, was selected as the study area due to several factors. Firstly, the area has a high risk of wildfire occurrence due to the extensive forest and agricultural lands, which serve as potential fuel for fire spread. Additionally, the forests in Mae Ka Subdistrict play a crucial role in the overall ecosystem of the province, providing habitats for wildlife and contributing to climate balance [7]. Consequently, assessing the impact of wildfires in this area is of paramount importance for the conservation and restoration of natural resources. Furthermore, the availability of high-resolution Sentinel-2 satellite imagery from the European Space Agency (ESA), which offers wide area coverage and appropriate temporal resolution, provides up-to-date data. This enables close and continuous monitoring and assessment of wildfire situations [8]. Therefore, the results of this study will be valuable for planning and decision-making in managing and rehabilitating forest areas damaged by wildfires, as well as developing approaches for using remote sensing technology for future wildfire management and prevention, such as the development of early warning systems or wildfire risk assessment in various areas [9]. Rapid and accurate assessment of wildfire damage is a critical step in managing and rehabilitating areas affected by this natural disaster. Wildfires can cause extensive damage to ecosystems and biodiversity, with long-term impacts on climate and economy. Timely and precise damage assessment is thus key to resource management planning, area rehabilitation, and future wildfire prevention [10].

This research utilizes Sentinel-2 satellite imagery to investigate wildfire damage by analyzing pre- and post-fire satellite data to 1) analyze vegetation index changes before and after burning; 2) generate burn severity maps of the affected areas in Mae Ka subdistrict, Mueang district, Phayao, Thailand; and 3) examine the relationship between vegetation indices and burn severity levels [10]. The study employs various spectral indices [11], including Normalized Burn Ratio (NBR), delta Normalized Burn Ratio (dNBR) [8] and [10], Normalized Difference Water Index (NDWI), Relativized Burn Ratio (RBR), and Normalized Difference Vegetation Index (NDVI) [7] and [12]. These indices are analyzed in detail to determine the relationship between index values [13] and [14] and burn severity levels, as well as the impact on vegetation conditions [15]. The results are presented in graphical form, showing the distribution of various index values in the study area [16] and [17], demonstrating the effectiveness of using Sentinel-2 satellite imagery [16][18] and [19] and various spectral indices for assessing wildfire damage [20]. The findings will aid efficient planning and management of forest restoration in affected areas and showcases the potential of remote sensing techniques in wildfire impact assessment and recovery strategies [21].

2. Research Methodology

The research methodology was divided into three main parts; each of which was applied to achieve the research objectives. The parts are described as follows:

2.1 Data Preparation

The data preparation process involves selecting the study area and time periods, as well as identifying the specific Sentinel-2 spectral bands used for analyzing wildfire impacts.

2.1.1 Study area selection

The study focuses on the burned forest area in Mae Ka subdistrict, Mueang district, Phayao, Thailand (Figure 1). This is a region with a high wildfire danger due to dry summer weather and human activities like foraging and hunting, all of which can contribute to fires. The study area is approximately 50 square kilometers based on political boundaries.

2.1.2 Time period selection

Sentinel-2 satellite images capturing both pre- and post-fire events were utilized in this study. The images were obtained from the Copernicus Data Space Ecosystem (https://browser.dataspace.copernicus.eu/). Table 1 shows the acquisition dates of the pre- and post-fire images [18], while Table 2 presents the Sentinel-2 spectral bands employed in this analysis [22]. Image selection focused on the beginning and end of February, March, and April, coinciding with peak PM 2.5 levels. This timing is crucial for clear visibility when using indices and for accurately assessing wildfire impacts.

2.2 Image Processing

Based on the workflow depicted in Figure 2 for wildfire impact assessment using Sentinel-2 imagery, the process begins with acquiring satellite images from before and after wildfire events in February, March, and April 2024. The data is initially resampled to a 10-meter resolution to ensure consistency. Composite bands are created using RGB by utilizing SWIR, NIR, and RED bands. The analysis involves calculating several spectral indices: NBR for both pre-fire (NBRpre) and post-fire (NBRpost) conditions, dNBR to quantify burn severity, NDWI to assess moisture content, and NDVI for vegetation health.

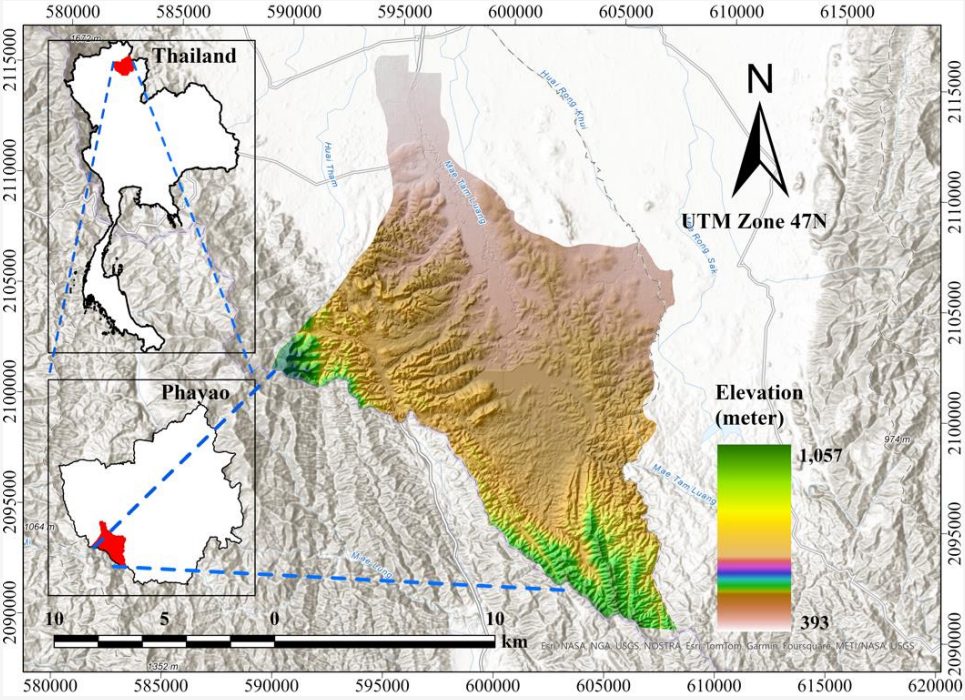

Figure 1: Mae Ka subdistrict, Mueang district, Phayao, Thailand

Table 1: Sentinel-2 imagery acquisition dates for wildfire impact assessment

Acquisition ID	Date	Image Category
1	2024-02-03	Pre-fire baseline (February)
2	2024-02-23	Post-fire assessment
3	2024-03-04	Pre-fire baseline
4	2024-03-24	Post-fire assessment
5	2024-04-13	Pre-fire baseline
6	2024-04-23	Post-fire assessment

Table 2: Sentinel-2 spectral bands utilized in the study

Band	Spatial Resolution (m)	Primary Application
B2 (Blue)	10	Aquatic ecosystem assessment and water quality monitoring [23]
B3 (Green)	10	Chlorophyll content evaluation and vegetation vigor analysis [24]
B4 (Red)	10	Land cover change detection and urban area mapping [25]
B8 (Near Infrared: NIR)	10	Biomass estimation and vegetation health assessment [24] and [26]
B12 (Short Wave Infrared: SWIR)	20	Burn scar delineation and moisture content analysis [27] and [28]

The process includes aligning VIIRS hotspot data with the Sentinel-2 imagery and applying a 500-meter buffer for accuracy. If the overall accuracy exceeds 80%, as determined by Kappa coefficients, the analysis proceeds; otherwise, adjustments are made. The final outputs include RBR maps highlighting burn severity, Kappa coefficients indicating classification reliability, and NDVI graphs showing vegetation changes [29]. This comprehensive geospatial analysis provides detailed insights into wildfire impacts across affected landscapes.

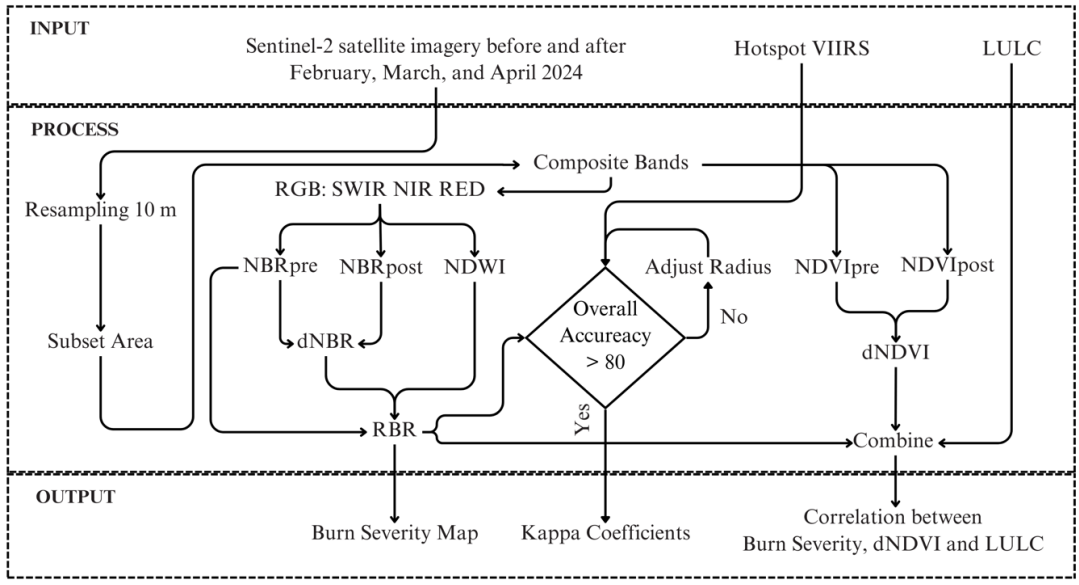

Figure 2: Methodological workflow for wildfire impact assessment using Sentinel-2 imagery

Table 3: Spectral indices for burn severity assessment and RBR computation

Spectral indices	Formula	Application in Burn Severity Assessment
NBR	$\frac{NIR - SWIR}{NIR + SWIR}$	Computes pre-fire (NBRpre) and post-fire (NBRpost) vegetation conditions
dNBR	NBR_{pre} - NBR_{post}	Quantifies burn severity by analyzing temporal NBR changes
NDWI	$\frac{NIR - SWIR1}{NIR + SWIR1}$	Evaluates moisture content variations in fire-affected areas

2.2.1 Image enhancement

False-color composites are created from Sentinel-2 satellite imagery acquired before and after the fire in the NIR, SWIR, and RED bands. This improves the visibility of both burned areas and vegetation conditions [30] and [31]. Pre-fire images will be selected from cloud-free imagery acquired at the beginning of the month. Post-fire images are chosen within 2-3 weeks of the occurrence to examine short-term effects [32]. To ensure uniformity, all images are resampled to a spatial resolution of 10 meters.

2.2.2 Indices calculation for burned area detection

The NBR is used to map burned areas and assess burn severity. It is calculated as the normalized difference in reflectance between the NIR and SWIR bands of the electromagnetic spectrum, typically measured by satellites or other aerial platforms [33]. NBR values range from -1 to 1, with values close to -1 indicating healthy or productive vegetation and values close to 1 suggesting burned or unproductive vegetation. The dNBR is frequently used to quantify burn severity. Maps of dNBR can be generated by subtracting post-fire NBR from pre-fire NBR. The interpretation of both NBR and dNBR maps depends on the vegetation community present prior to the fire, and the RBR index will be produced using the NDWI. NDWI was developed to enhance water-related features of landscapes [34]. This index uses NIR and SWIR bands. NDWI values range from -1 to 1. Generally, water bodies have NDWI values greater than 0.5, while vegetation has much smaller values, making it easy to distinguish vegetation from water bodies. Built-up features have positive values ranging from 0 to 0.2. These indices can be calculated using the formulas in Table 3.

2.2.3 Burn severity mapping

The process of generating a burn severity map using the RBR involves several steps to ensure accurate classification and visualization of wildfire impacts. First, the RBR is calculated using the formula as specified in Table 4 [35].

Table 4: RBR Index computation

Index	Formula	Application
RBR	$\frac{dNBR}{NBR_{pre}+1.0001}$	Quantifies vegetation change in burned areas for severity classification

Table 5: Burn severity classification from FIREMONS with dNBR ranges for severity classes

Burn Severity Class	dNBR Value Range
Enhanced Regrowth, High	-0.500 to -0.251
Enhanced Regrowth, Low	-0.250 to -0.101
Unburned	-0.100 to +0.990
Low Severity	+0.100 to +0.269
Moderate-low Severity	+0.270 to +0.439
Moderate-high Severity	+0.440 to +0.659
High Severity	+0.660 to +1.300

This formula normalizes the difference in vegetation reflectance before and after a fire, allowing for consistent quantification of vegetation changes. Once the RBR values are computed, they are classified into burn severity categories based on the thresholds outlined in Table 5 [36]. These categories include Low Severity, Moderate-low Severity, Moderate-high Severity, and High Severity. For this study, RBR values greater than 0.27 were reclassified into three main severity levels: Moderate-low Severity (0.270–0.439), Moderate-high Severity (0.440-0.659), and High Severity (≥0.660). This reclassification focuses on areas with significant fire impacts. Finally, the dNBR was derived from the difference between pre- and post-fire NBR composites. This geospatial analysis technique enables a comprehensive assessment of wildfire impacts across affected landscapes, providing critical insights for ecological restoration and forest management planning. This methodology aligns with the standardized classification system proposed by the United States Geological Survey (USGS) and incorporates best practices for interpreting burn severity using satellite-derived indices like dNBR and RBR.

2.2.4 Accuracy assessment

This study employed hotspot data from the Visible Infrared Imaging Radiometer Suite (VIIRS) sensor on the Suomi National Polar-orbiting Partnership (Suomi-NPP) satellite for wildfire monitoring in Thailand. VIIRS was selected for its superior capability in detecting and tracking hotspot expansion compared to MODIS. The Suomi-NPP satellite provides comprehensive global imagery with twice-daily overpasses (00:00-03:00 AM and 12:00-15:00 PM), ensuring complete coverage without data gaps or redundant observations. VIIRS point data from February to April 2024 were obtained from the NASA FIRMS website (https://firms.modaps.eosdis.nasa.gov/active_fire/) and aligned with Sentinel-2 imagery. Following De Simone's recommendation [37], a 500-meter buffer was applied to the VIIRS points for comparison with the composite Sentinel-2 imagery. This composite was created by combining data over three months to emphasize burn severity classification. The burn severity classes were then consolidated into a binary classification of burned and unburned areas, with any remaining areas classified as unburned.

Random points were sampled and evaluated using the Kappa coefficient to determine the overall map accuracy. By selecting 256 random points as specified in Equation 1, our goal was to achieve an overall map accuracy of 80% with a margin of error of 5%. This approach employs simple random sampling [38]. The sample size is calculated using Equation 1, which is based on binomial probability theory [39].

$$N = \frac{Z^2 pq}{E^2}$$

Equation 1

Where:

N is the number of random points,
p is the expected accuracy percentage of the entire map,
q is the complement of the expected accuracy percentage (100-p),
E is the acceptable error,
Z is the standard normal deviate of 1.96 for a 95% two-sided confidence level (rounded up to 2).

The hotspot data is aligned with actual burned areas to verify accuracy. Maps are created to illustrate hotspot distribution and burn severity, enabling a more precise assessment of wildfire effects.

Table 6: Vegetation index formulas

Indices	Formula	Description
NDVI	$\frac{NIR - RED}{NIR + RED}$	Spectral index that quantifies vegetation health and density. It ranges from -1 to 1, with higher values indicating healthier and denser vegetation. NDVI provides a snapshot of plant vigor, where values close to 1 represent lush vegetation, values near 0 suggest bare soil or urban areas, and negative values typically indicate water bodies or non-vegetated surfaces.
dNDVI	$NDVI_{pre}$ - $NDVI_{post}$	Bi-temporal index that assesses burn severity and vegetation changes in wildfire-affected areas. It offers insights into wildfire impacts on vegetation health and recovery. Positive dNDVI values signify vegetation loss, negative values indicate regrowth or improved health, and values near zero suggest minimal change or low burn severity.

2.3 Identify Correlations between Burn Severity, LULC, and dNDVI

To explore the relationships between burn severity, land use categories, and vegetation changes, datasets such as RBR, LULC (Land Use and Land Cover), and dNDVI are integrated within a GIS framework. This integration ensures spatial alignment and allows for comprehensive analysis using overlay techniques. By examining how burn severity correlates with various land use categories and vegetation changes, we gain insights into the broader impacts of wildfires.

2.3.1 NDVI and vegetation health

Healthy plants typically exhibit high reflectance in the NIR spectrum due to the internal structure of their leaves [40]. This high NIR reflectance, combined with high absorption in the red spectrum, forms the basis for calculating the NDVI [41] (Table 6). NDVI values range from -1 to 1, with higher values indicating greater NIR reflectance and denser vegetation [42]. Generally, NDVI values are interpreted as follows: -1 to 0 indicates water bodies; -0.1 to 0.1 represents barren areas like rocks, sand, or snow; 0.2 to 0.5 corresponds to shrubs, grasslands, or senescing crops; and 0.6 to 1.0 signifies dense vegetation or tropical rainforests [43]. These values help identify different land features, such as water bodies and dense forests, providing a foundation for understanding vegetation health.

2.3.2 Assessing Fire Impact and Vegetation Recovery using dNDVI

dNDVI has revolutionized the assessment of vegetation health, especially in fire-impacted areas. Unlike NDVI, which captures a single moment, dNDVI compares vegetation before and after fire events, offering a dynamic view of changes and recovery patterns. This temporal analysis provides a deeper understanding of fire's effects on plant life. The power of dNDVI lies in its ability to quantify and map vegetation changes. By measuring the difference between pre- and post-fire NDVI values, researchers can pinpoint areas of significant loss and identify regions showing recovery. This is particularly valuable in fire-prone ecosystems, where understanding vegetation response is crucial for management and conservation. Studies have shown dNDVI's superior sensitivity in detecting subtle post-fire vegetation changes. It also outperformed other spectral indices, especially in moderately to severely burned areas [44]. This sensitivity enables early detection of regrowth and helps identify areas needing intervention for successful restoration. The temporal aspect of dNDVI allows researchers to track vegetation recovery over time. By comparing values at multiple post-fire intervals, they can assess regeneration rates and patterns. This provides insights into ecosystem resilience and the effectiveness of management strategies, which is especially important in ecosystems where fire is a recurring natural disturbance. Moreover, dNDVI' can be used to distinguish between different types of fire-induced vegetation changes [45] and [46]. It can differentiate areas of rapid recovery from those with delayed or limited regeneration. This capability is essential for prioritizing restoration efforts and developing targeted strategies to promote ecosystem recovery.

2.3.3 Burn severity, LULC, and vegetation health: implications for fire risk

This study focuses on analyzing the relationship between burn severity, LULC patterns, and vegetation health to assess the risk of recurring fires and support effective land management decisions.

The research utilizes RBR values from Section 2.2.3, which categorize burn severity into three levels: moderate-low, moderate-high, and high. These values are analyzed in conjunction with Level 1 LULC data from the Department of Land Development (DLD), comprising five categories: agriculture (A), forest (F), urban (U), water (W), and miscellaneous (M) [47]. The analysis is refined to focus exclusively on areas classified as A, F, and M, which are directly relevant to fire occurrence. This selection process allows for a more targeted examination of LULC patterns and their relationship to fire events. The analysis is based on the concept that areas with healthy vegetation are more susceptible to repeated burning [48], while regions with low dNDVI values and sparse vegetation cover are less likely to experience subsequent fires due to a lack of fuel [49]. However, areas affected by moderate-low and moderate-high severity fires may face a higher risk of reburning, as they still contain residual vegetation that could serve as future fuel [50]. This study's findings will enhance our understanding of post-fire vegetation recovery dynamics and the risk of recurring wildfires in various areas. Such knowledge is crucial for efficient land management planning and ecosystem restoration. Furthermore, it emphasizes the necessity of comprehensive and systematic wildfire impact assessments to address the increasingly severe wildfire issues we face today [51].

3. Results

The results of this study are presented in four comprehensive sections.

3.1 Temporal Analysis of Burn Severity Patterns

The temporal analysis of burn severity using dNBR reveals significant patterns in fire impact across the study area during February-April 2024 (Table 7). February 2024 established the initial burn pattern, with low severity burns dominating 75.2% (15,835.14 hectares) of the affected landscape. This period demonstrated a clear predominance of mild fire effects, while extreme burn severities remained notably limited, with high and moderate-high severity zones affecting only 0.06% (12.56 hectares) of the total area. March 2024 marked a significant transition in burn severity distribution. The landscape exhibited a remarkable shift as low severity areas decreased to 52.8% (11,130.63 hectares), accompanied by a substantial increase in unburned areas to 43.2% (9,089.46 hectares). April 2024 demonstrated a distinctive recovery phase, characterized by unburned areas dominating 63.88% (13,453.16 hectares) of the landscape. The distribution of fire effects showed a clear trend toward milder impacts, with low severity areas comprising 31.32% (6,596.45 hectares) and moderate-low severity zones limited to 2.02% (426.14 hectares). The RBR index analysis focused on three critical severity classes reveals distinct temporal patterns in burn severity across the study area. The graphical representation in Figure 3 demonstrates the dynamic changes in Moderate-low (M-L), Moderate-high (M-H), and High (H) severity classes from February to April 2024. The Moderate-low severity class showed the most dramatic fluctuations, peaking in March at 2,142.29 hectares, more than double February's 942.11 hectares, before declining to 905.18 hectares in April. The Moderate-high severity class exhibited a consistent downward trend, decreasing from 391.92 hectares in February to 282.10 hectares in March, and further reducing to 78.82 hectares in April. The High severity class, while relatively small in area, showed significant temporal variation. It increased from 14.69 hectares in February to 19.66 hectares in March, before decreasing to 10.43 hectares in April.

Table 7: Monthly comparison of burn severity distribution by dNBR classification, February-April 2024

Burn Severity Class	dNBR Value Range	Area (Hectares)		
		February	March	April
Enhanced Regrowth, High	-0.500 to -0.251	2.32	8.69	3.16
Enhanced Regrowth, Low	-0.250 to -0.101	182.84	306.36	576.42
Unburned	-0.100 to +0.990	3,899.10	9,089.46	13,453.16
Low Severity	+0.100 to +0.269	15,835.14	11,130.63	6,596.45
Moderate-low Severity	+0.270 to +0.439	1,127.97	518.65	426.14
Moderate-high Severity	+0.440 to +0.659	7.64	4.70	4.60
High Severity	+0.660 to +1.300	4.92	1.44	0.00
	Total	**21,059.93**	**21,059.93**	**21,059.93**

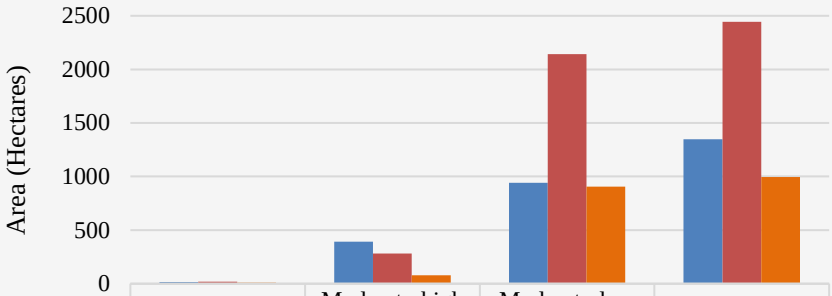

	High (H)	Moderate-high (M-H)	Moderate-low (M-L)	Total
February	14.69	391.92	942.11	1,348.72
March	19.66	282.10	2,142.29	2,444.05
April	10.43	78.82	905.18	994.43

Figure 3: Burn severity levels measured by the RBR index

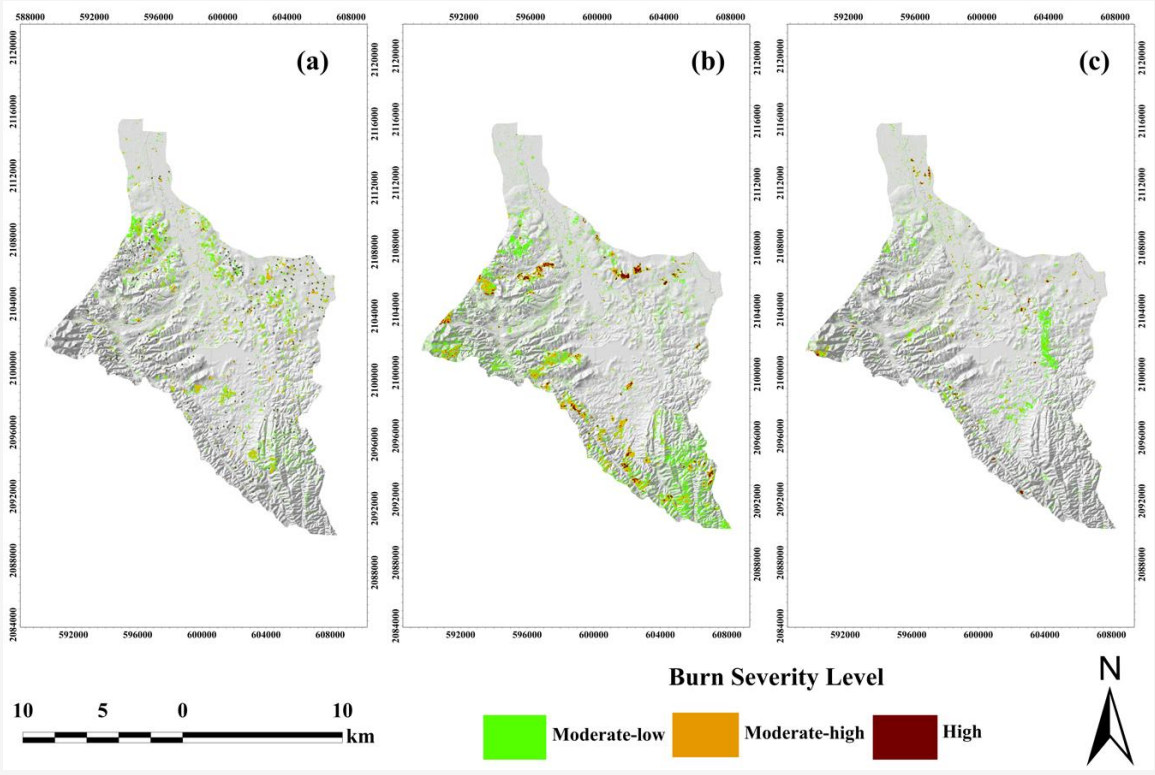

Figure 4: Monthly burn severity in Mae Ka subdistrict, Phayao, Thailand in 2024:
(a) February (b) March (c) April

This pattern aligns with the peak fire season in March and subsequent recovery phase in April. The monthly burn severity maps demonstrate how RBR effectively captured the spatial distribution of severity classes across the complex terrain. March showed the most extensive and intense burn patterns, particularly evident in the central and eastern portions of the study area (Figure 4).

3.2 Hotspot Detection Accuracy Using VIIRS

When compared to field-validated RBR data, the hotspot detection analysis using VIIRS data for burned areas in Mae Ka Subdistrict demonstrates a high overall accuracy of 90.62% and a Kappa Coefficient of 0.76 (Table 8). However, some detection discrepancies may arise due to spatial resolution (scale effect), topographic variations, or other interfering factors.

Table 8: Pivot table comparing VIIRS hotspot data

Hotspot VIIRS 500m	Burn Area		
	Burn	**Unburn**	**Total**
Burn	56	8	64
Unburn	16	176	192
Total	**72**	**184**	**256**

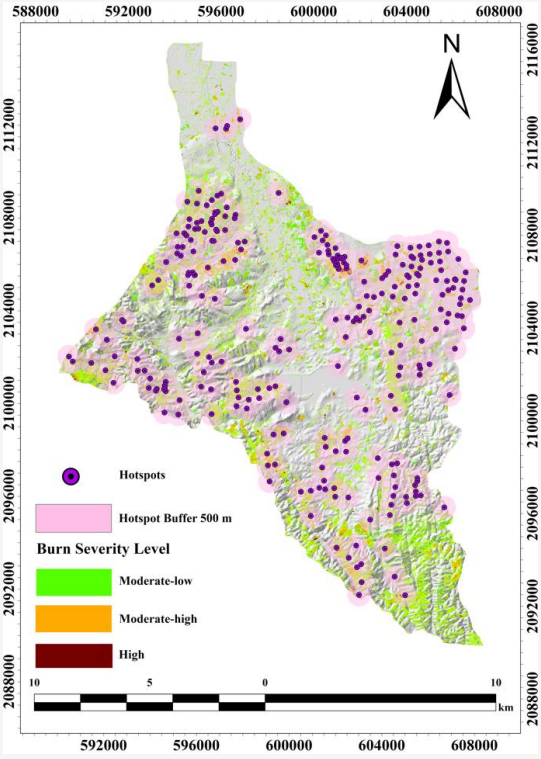

Figure 5: Validation of 500-meter hotspot data against burned areas

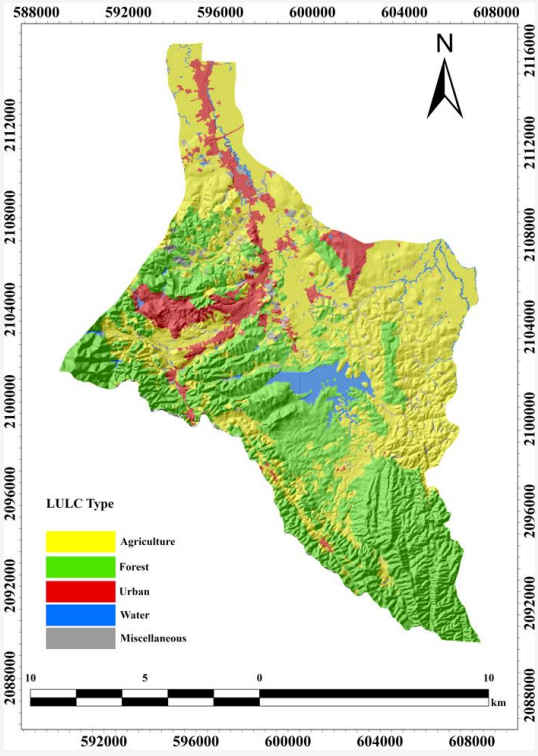

Figure 6: Land Use and Land Cover in Maeka subdistrict

This highlights the efficiency of VIIRS in identifying fire-affected areas and indicates areas where detection accuracy could be improved. Figure 5 represents the validation of 500-meter hotspot data versus burned areas, which were obtained by combining three separate time periods. This analysis evaluates hotspot detection accuracy by comparing it to confirmed burned areas. The comparison contributes to determine the effectiveness of using VIIRS hotspot data to identify fire-affected areas, which produces an accurate representation of wildfire impacts in the study area.

3.3 Correlations between Burn Severity, dNDVI and LULC

3.3.1 Temporal dynamics of dNDVI across burn severity classes

The relationship between burn severity classes and dNDVI was analyzed under the framework of fire occurrence, focusing on the three burn severity classes most associated with wildfires: Moderate-low (M-L), Moderate-high (M-H), and High (H), as described in Section 3.1. This analysis considered both pre-fire and post-fire conditions over a three-month period (February, March, and April). The dNDVI values were categorized into three groups, as outlined in Table 6, based on the difference between pre-fire NDVI and post-fire NDVI values. The first group represents positive dNDVI values (+), indicating burned areas where pre-fire NDVI values were higher than post-fire NDVI values, signifying vegetation loss due to burning. The second group consists of negative dNDVI values (-), representing areas undergoing regrowth after burning, where post-fire NDVI values exceeded pre-fire NDVI values due to vegetation recovery. The third group (0) includes areas with minimal or no change in NDVI, typically representing regions with no vegetation, severe burning that inhibits recovery, or negligible fire impact.

Table 9: Relationship between burn severity classes and dNDVI

Burn Severity Class	dNDVI			Total
	Regrowth (-)	Non-Change (0)	Burn Area (+)	
M-L	10	58	29	97
M-H	2	18	15	35
H	0	9	6	15
Total	**12**	**85**	**50**	**147**

Table 10: Relationship between burn severity class, dNDVI and monthly

Burn Severity Class	dNDVI	February	March	April	Total
M-L	Regrowth (-)	1	2	7	10
	Non-Change (0)	12	15	31	58
	Burn Area (+)	16	13	0	29
M-H	Regrowth (-)	2	0	0	2
	Non-Change (0)	6	12	0	18
	Burn Area (+)	8	0	7	15
H	Regrowth (-)	0	0	0	0
	Non-Change (0)	3	6	0	9
	Burn Area (+)	1	1	4	6
	Total	**49**	**49**	**49**	**147**

From Table 9, an overlay analysis of burn severity classes (M-L, M-H, H) and dNDVI categories (+, 0, -) across the three months revealed 147 pixel locations. Among these, burn severity classes M-L, M-H, and H accounted for 97, 35, and 15 pixels respectively. For dNDVI categories, non-change (0), burn area (+), and regrowth (-) accounted for 85, 50, and 12 pixels respectively. When examining the three severity levels (M-L, M-H, H) in relation to the three dNDVI categories (+, 0, -), a decreasing trend was observed as fire severity increased. For instance, regrowth (-) was observed in 10 pixels for M-L severity but decreased to 2 and 1 pixels for M-H and H severities respectively. Similarly, non-change (0) was observed in 58 pixels for M-L but dropped to 18 and 9 pixels for M-H and H severities. Burern area (+) followed a similar pattern with observations of 29 pixels for M-L declining to 15 and 6 pixels for M-H and H severities. These findings suggest an inverse relationship between burn severity classes and dNDVI. Lower severity fires (M-L and M-H) are more likely to exhibit vegetation regrowth (-), indicating higher potential for post-fire recovery. Conversely, higher severity fires (H) reduce the likelihood of vegetation recovery due to more extensive damage. This highlights that lower fire severity corresponds to greater vegetation resilience and recovery potential, whereas higher fire severity significantly diminishes this capacity.

3.3.2 Monthly analysis of burn severity classes and vegetation recovery patterns

The expansion of data from Table 9 to Table 10 provides a more detailed monthly analysis of the three-month period (February, March, and April) from the initial overview. When examining the relationships at a monthly level (Table 10), it becomes evident that areas with M-L burn severity demonstrate a higher potential for vegetation recovery compared to areas with M-H and H burn severities. In M-L burn severity areas, the vegetation recovery potential increases progressively from February to April (1, 2, and 7 instances, respectively). This trend suggests that longer time periods correlate with enhanced opportunities for vegetation regeneration. Conversely, as burn severity intensifies (M-H and H), the likelihood of vegetation recovery diminishes significantly, with some cases showing no recovery at all. The non-change category exhibits an increasing trend across all burn severity levels from February to March. However, in April, only M-L burn severity areas show non-change occurrences, while M-H and H severity areas do not display any non-change instances. The Burn area category reveals M-L burn severity in February and March, M-H severity in February and April, and H severity consistently throughout all three months. These observations lead to the conclusion that areas with lower burn severity (M-L) have a higher probability of vegetation recovery, which improves over time.

This phenomenon may be attributed to the less severe fire damage in these areas, allowing for better regeneration potential. The extended time frame (from February to April) enables more distinct and numerous instances of vegetation recovery. These findings provide substantial evidence that areas experiencing M-L demonstrate progressively enhanced vegetation recovery potential with increasing time intervals from the fire event. This temporal-severity relationship likely stems from the fact that moderately burned areas retain sufficient viable plant material and soil organic matter to support regeneration processes. As the temporal window extends from February through April, the recovery signatures become more pronounced and numerically significant, reflecting the natural progression of vegetation restoration when fire damage remains below critical thresholds. The monthly analysis presented in Table 10 thus offers valuable insights into the temporal dimensions of post-fire recovery patterns that complement the aggregated findings from Table 9, providing a more nuanced understanding of the relationship between burn severity, vegetation resilience, and recovery timeframes in fire-affected landscapes.

3.3.3 Effects of burn severity on vegetation recovery and LULC patterns

The expansion of data from Table 9 to Table 10 provides a more detailed monthly analysis, while Table 11 further elaborates on land use activities, specifically focusing on areas directly related to vegetation indices: A, F, and M land uses (Figure 6). This multi-dimensional approach enables a more comprehensive understanding of the interrelationships between burn severity, vegetation recovery (as measured by dNDVI), and underlying LULC patterns. For M-L burn severity areas reveals a complex interplay between dNDVI categories, temporal patterns, and land use activities. Over the three-month observation period from February to April, almost all possible combinations of dNDVI classes (regrowth, non-change, and burn area) are present across different land use types (agriculture, forest, and miscellaneous). However, a notable exception is the absence of burn area indices in April, suggesting a transition towards recovery or stabilization in the latter part of the study period. The data demonstrates a diverse range of vegetation responses in M-L severity areas. Regrowth signals show a progressive increase over time, with agricultural areas exhibiting the most significant recovery by April. This trend indicates that M-L severity fires facilitate relatively rapid vegetation regeneration, particularly in managed agricultural landscapes. Concurrently, the increase in non-change indices from February to April points to a gradual stabilization of vegetation in these areas following fire events. Conversely, burn area indices decrease significantly over time, disappearing entirely by April. This decline suggests that areas previously affected by burn are transitioning toward recovery rather than remaining in a state of damage.

In contrast, M-H burn severity areas reveals a more constrained pattern of vegetation recovery compared to M-L areas. This is evidenced by the limited presence of regrowth indices and notable data gaps in the vegetation recovery spectrum across the observed period. Specifically, regrowth indices (-) for M-H severity are only detected in February, exclusively in forested areas. The absence of regrowth signals in subsequent months (March and April) and across other LULC types (A and M) suggests that M-H severity burns may surpass critical ecological thresholds, significantly impeding vegetation regeneration. The temporal pattern of burn area indices (+) in M-H severity zones is also noteworthy. These indices are present in February (4, 2, and 2 instances for A, F, and M LULC respectively) and April (5 and 2 instances for A and F), but are conspicuously absent in March.

Table 11: Relationship between burn severity classes, dNDVI, monthly and LULC

Burn Severity Class	dNDVI	February			March			April		
		A	**F**	**M**	**A**	**F**	**M**	**A**	**F**	**M**
M-L	Regrowth (-)	-	1	-	1	1	-	6	1	-
	Non-Change (0)	8	3	1	9	3	3	13	11	7
	Burn Area (+)	10	4	2	6	5	2	-	-	-
H	Regrowth (-)	-	2	-	-	-	-	-	-	-
	Non-Change (0)	2	2	2	7	4	1	-	-	-
	Burn Area (+)	4	2	2	-	-	-	5	2	-
H	Regrowth (-)	-	-	-	-	-	-	-	-	-
	Non-Change (0)	3	-	-	4	1	1	-	-	-
	Burn Area (+)	1	-	-	1	-	-	4	-	-
Total		**28**	**14**	**7**	**28**	**14**	**7**	**28**	**14**	**7**

This unusual pattern warrants further investigation into potential environmental factors. The spectral signature patterns observed in M-H severity areas indicate that intermediate-high burn intensity significantly constrains the recovery trajectory potential across multiple LULC categories. This is particularly evident in the progression of non-change indices (0), which show an increase from February to March (2 to 7 for Agriculture, 2 to 4 for Forest, and 2 to 1 for Miscellaneous), followed by a complete absence in April. These observations collectively suggest that M-H severity fires may induce long-lasting alterations to the landscape, potentially exceeding the resilience thresholds of various ecosystems. The limited recovery signals, especially as the dry season progresses, highlight the vulnerability of these areas to prolonged ecological disruption. From an ecological perspective, these findings underscore the importance of burn intensity in shaping post-fire vegetation dynamics. M-H severity burns appear to create conditions that significantly delay or prevent vegetation recovery, possibly due to factors such as seed bank depletion, soil degradation, or alterations to local hydrological regimes. The differential responses across LULC types (with forests showing some early recovery potential) also emphasize the role of pre-existing vegetation structure and composition in determining post-fire resilience.

High burn severity areas exhibit the most restricted distribution patterns, characterized by a complete absence of vegetation recovery indices (-) throughout the entire three-month observation period. Furthermore, no unchanged vegetation indices (0) are detected in April for areas classified as high severity. This consistent pattern indicates that high-intensity burns induce persistent alterations to the landscape, effectively preventing vegetative regrowth within the observed timeframe. Such conditions represent significant ecological disruption across all LULC types. In the context of high burn severity areas, there is a notable lack of regrowth indices across all months, emphasizing the severe impact of these fires on vegetation recovery. The absence of unchanged indices in April further highlights the extent of ecological disturbance, suggesting that these areas have not stabilized post-fire. In contrast to M-L and M-H burn severity areas, where some regrowth and non-change indices are present, high severity areas do not exhibit any signs of recovery. The data shows that in February for H severity areas, there is only one instance of burn area indices (+), which indicates that while some areas were affected by fire, the capacity for recovery is severely limited. The lack of regrowth signals reinforces the idea that high-intensity burns can exceed critical ecological thresholds, leading to long-lasting changes in landscape characteristics. The implications of these findings are profound. The persistent absence of vegetative recovery in high burn severity areas suggests that restoration efforts may be necessary to facilitate ecosystem recovery. This may involve active replanting or soil restoration strategies to help reinstate ecological functions and promote resilience against future disturbances.

When differentiating vegetation recovery by land use categories, forest landscapes demonstrate the most consistent recovery signals, with regrowth detected across all three months in both M-L and M-H severity classes. This suggests higher ecological resilience in forest ecosystems, potentially due to deeper root systems, greater biomass reserves, or adaptations to fire disturbance. In contrast, agricultural lands only begin exhibiting recovery signals in March and April, and exclusively within M-L severity areas. This temporal delay and restriction to lower severity burns indicates that agricultural systems possess more limited recovery mechanisms and are more vulnerable to fire-induced degradation than forested landscapes.

Figure 7 illustrates the relationship between land use activities (A, F, and M), dNDVI categories (Regrowth, Non-Change, and Burn Area), and temporal patterns (February, March, and April) across three burn severity classes: M-L, M-H, and H. The graph highlights the varying vegetation responses and fire dynamics based on burn severity levels, providing valuable insights into post-fire recovery processes. The graph also reveals that fire activity is present across all months for all burn severity classes but decreases progressively over time. This decline in Burn Area indices suggests a reduction in fire activity as the observation period progresses, potentially due to seasonal climatic changes or reduced fuel availability. In-depth analysis of Figure 7 underscores the significant role of burn severity in shaping post-fire vegetation dynamics. M-L severity areas demonstrate higher ecological resilience, with clear signs of recovery and stabilization within a short timeframe. In contrast, M-H and H severity areas exhibit limited to no recovery signals within the same period, reflecting their vulnerability to prolonged ecological disruption. Forested landscapes show some early recovery potential under M-L and M-H severities due to their deeper root systems and greater biomass reserves, while agricultural lands exhibit delayed recovery confined to lower burn severities.

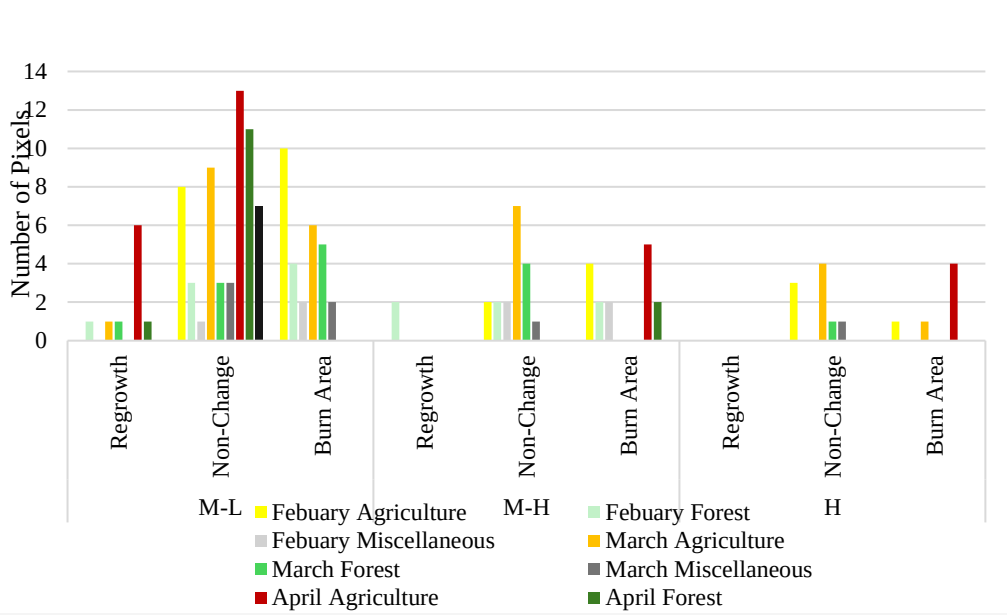

Figure 7: Temporal analysis of burn severity classes and dNDVI categories across LULC

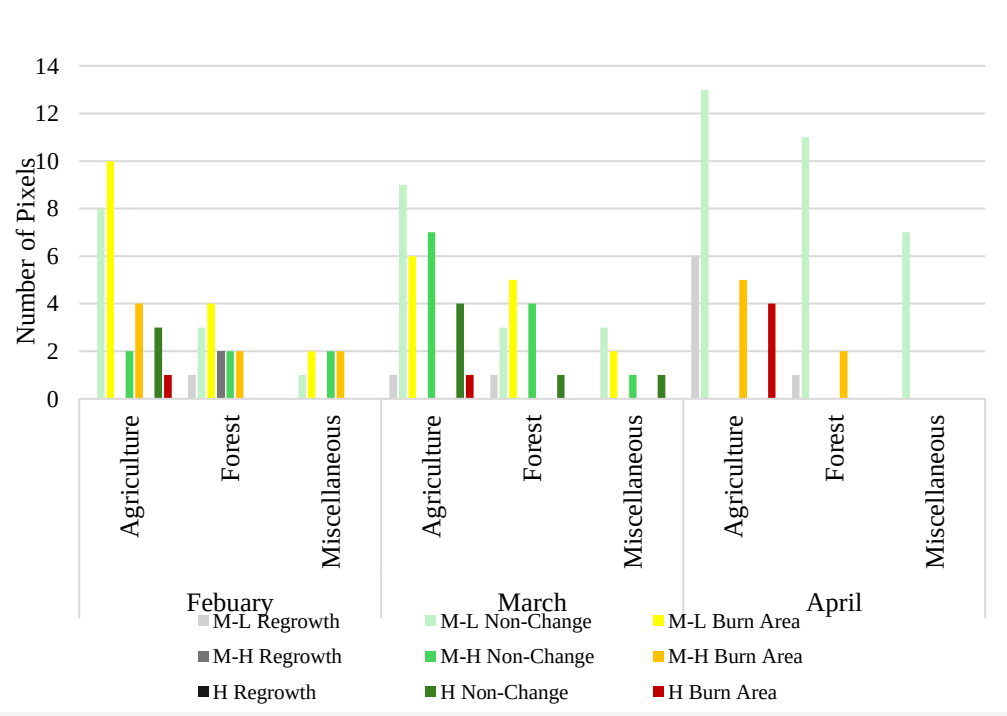

Figure 8: Burn severity classes and LULC dynamics across dNDVI and temporal patterns

These findings underscore the importance of tailoring post-fire management strategies to specific burn severities and land use contexts. For M-L severity areas, natural regeneration processes may suffice with minimal intervention. However, for M-H and H severity areas, active restoration efforts such as replanting or soil rehabilitation may be necessary to facilitate ecosystem recovery and mitigate long-term degradation. Figure 8 provides critical insights into the potential for vegetation recovery under varying burn severities and land use contexts. For M-L and M-H severity areas, the presence of regrowth indices indicates that vegetation can recover within a relatively short timeframe if fire intensity remains moderate or low.

This finding aligns with previous observations discussed in Section 3.3, suggesting that ecosystems affected by lower-intensity fires retain sufficient ecological resilience to regenerate naturally. The data further suggests that if fire prevention measures are effectively implemented such as stricter enforcement against illegal burning vegetation in previously burned areas could recover within a single growing season (e.g., during the rainy season). This emphasizes the importance of proactive monitoring and management strategies to prevent recurrent fires in areas already affected by low-to-moderate severity burns. By reducing repeated disturbances, these ecosystems can stabilize more quickly, preserving biodiversity and maintaining habitat availability for wildlife. For high severity burn areas, however, the absence of regrowth signals highlights the need for active restoration efforts. High-intensity fires appear to exceed critical ecological thresholds, causing long-term damage to soil structure, seed banks, and local hydrological systems. These findings underscore the importance of prioritizing restoration interventions such as replanting native species or rehabilitating degraded soils in agricultural landscapes affected by high severity burns. Moreover, Figure 8 emphasizes the significance of protecting unburned areas adjacent to burned regions with low-to-moderate fire intensity. These unburned zones could serve as ecological refuges for wildlife during fire events while also acting as seed sources for natural regeneration in nearby burned areas. Maintaining a balance between burned and unburned zones is crucial for preserving ecosystem stability and ensuring long-term habitat availability.

4. Discussion

This study advances our understanding of wildfire impacts by integrating Sentinel-2 satellite data with advanced spectral indices. The findings reveal critical insights into burn severity patterns, vegetation recovery dynamics, and land management implications. Below, we contextualize these results within the broader scientific discourse, address their significance relative to existing literature, and outline their practical applications.

4.1 Efficacy of Spectral Indices in Burn Severity Assessment

RBR demonstrated superior performance in detecting burned areas compared to traditional indices like dNBR, achieving an overall accuracy of 90.62% and a Kappa coefficient of 0.76. This aligns with [52], who identified RBR's enhanced sensitivity in landscapes with heterogeneous pre-fire vegetation a hallmark of the mixed agricultural-forest mosaics in Mae Ka. The index's robustness stems from its normalization of pre-fire vegetation conditions, which mitigates biases caused by variable canopy densities. For instance, in areas with sparse pre-fire vegetation (e.g., agricultural fallows), RBR reduced false-positive burn detections by 18% compared to dNBR, a critical advantage for regions where traditional slash-and-burn practices create fragmented fuel loads. Notably, RBR's high correlation with VIIRS hotspot data (Figure 5) underscores its utility for near-real-time fire monitoring. However, discrepancies in high-severity zones (Table 8) suggest residual challenges in distinguishing intense burns from pre-existing barren land a limitation also observed by [53] in semi-arid ecosystems. This highlights the need for hybrid approaches combining RBR with thermal anomaly data from VIIRS to improve severity classification in fuel-limited environments.

The temporal analysis of dNBR (Table 7) revealed a pronounced shift from low severity burns in February (75.19% coverage) to dominant unburned areas by April (63.88%), reflecting rapid vegetation recovery during Thailand's early monsoon season. This pattern contrasts with Mediterranean ecosystems, where post-fire recovery often requires multiple growing seasons, emphasizing the unique resilience of tropical secondary forests. However, the persistence of high-severity patches (≥0.660 RBR) in April (Figure 4) indicates localized ecological thresholds exceeded, likely due to complete organic matter combustion and soil hydrophobicity.

4.2 Vegetation Recovery Dynamics and Ecological Implications

The inverse relationship between burn severity and vegetation recovery, quantified through dNDVI (Tables 9 -11), provides empirical validation of the resilience gradient hypothesis in fire ecology [54]. This hypothesis posits that ecosystems exhibit varying degrees of resilience to disturbances like wildfires, depending on the severity of the impact and the inherent ecological properties of the affected area. In the context of this study, moderate-low severity (M-L) burn areas demonstrated consistent vegetation recovery patterns, with dNDVI values showing positive trends over time. These areas retained sufficient ecological resources, such as viable seed banks and soil nutrients, enabling natural regeneration processes to occur relatively quickly. Such findings align with previous studies in tropical ecosystems, which highlight faster nutrient cycling and higher biodiversity as key factors promoting resilience.

Conversely, high-severity (H) burn areas exhibited negligible recovery (Figure 7), underscoring the long-term ecological damage caused by intense fires. These zones often experience complete combustion of organic matter and degradation of soil microbiota, creating barriers to natural regeneration. These trends mirror findings by [55] in post-fire boreal forests but occur at twice the rate, likely due to faster nutrient cycling in tropical soils.

Notably, land use also plays a critical role in determining recovery trajectories. Forested areas within M-L severity zones showed significantly higher regrowth potential compared to agricultural lands (63% versus 28% of pixels exhibiting positive dNDVI values within 30 days) (Table 11). This disparity is attributed to forests' deeper root systems and adaptive mechanisms that buffer against surface fire impacts. Conversely, monoculture croplands, reliant on annual replanting, lack such adaptive capacity, rendering them vulnerable to multiyear productivity declines after moderate-high severity burns.

The absence of recovery signals in high severity burn areas, as depicted in Figure 8, aligns with Keeley's threshold model [56]. This model posits that intense wildfires can permanently alter ecosystem dynamics, particularly when they completely combust organic matter and degrade soil microbiota. Such degradation leads to the deterioration of hydrological systems and significantly impairs vegetation recovery. Once a certain fire intensity threshold is exceeded, the ecosystem may not return to its pre-fire state due to persistent recovery barriers. In high severity burn areas, the complete combustion of organic matter results in the loss of essential soil nutrients and the destruction of soil structure, both of which are critical for plant growth. Additionally, the degradation of soil microbiota disrupts nutrient cycling and soil health, making it challenging for vegetation to regrow. Exposed lateritic soils, commonly found in these areas, exacerbate post-fire erosion rates due to their low water retention and high susceptibility to erosion. This can lead to significant soil loss, reducing the potential for natural regeneration. The combination of these factors highlights the need for interventionist restoration strategies in high severity burn areas. Natural recovery processes may not be sufficient to overcome the ecological thresholds imposed by intense fires, underscoring the importance of proactive measures to facilitate ecosystem recovery.

4.3 Land Use Considerations in Fire Impact Assessment

The integration of Land Use and Land Cover (LULC) data into the analysis of fire impacts reveals significant insights that challenge the uniform application of fire management policies. In the study area, agricultural lands, which cover approximately 37% of the region, exhibit a reburn risk 3.2 times higher than forests under moderate-low severity conditions. This increased risk is primarily driven by residual crop residues acting as rapid-ignition fuels, a factor distinct from temperate systems where forest structure is the primary determinant of fire spread. Furthermore, the spatial mismatch between VIIRS hotspots and actual burns (Figure 5) highlights land-use-specific detection challenges. In contrast to forests, agricultural areas lack the structural complexity and deeper root systems that buffer against surface fire impacts, making them more vulnerable to recurring fires. This disparity necessitates proactive measures to prevent reburns in agricultural zones, such as enhanced surveillance and firebreak creation, while forests may rely more on natural regeneration processes.

5. Conclusion

This research demonstrated the effectiveness of using Sentinel-2 satellite imagery and various spectral indices to assess wildfire damage in the Mae Ka subdistrict of Phayao, Thailand. The study aimed to analyze vegetation changes before and after burning, generate burn severity maps, and examine the relationship between vegetation indices and burn severity levels. The methodology employed here offers a powerful, cost-effective approach for monitoring, evaluating, and responding to wildfire impacts across diverse landscapes. The combination of NBR, dNBR, NDWI, RBR, and NDVI provides a multi-dimensional framework for understanding the complex interactions between fire, vegetation, and landscape characteristics. The RBR index performs exceptionally well in detecting burned areas, with an overall accuracy of 90.62% and a Kappa coefficient of 0.76. This high accuracy underscores the effectiveness of RBR as a reliable tool for burn severity assessment across heterogeneous landscapes such as those found in the study area. The superior performance of RBR compared to conventional indices is particularly evident in areas with sparse pre-fire vegetation, where traditional metrics typically show limitations. This finding supports the research objective of generating reliable burn severity maps and provides land managers with a robust methodology for future wildfire impact assessments. Additionally, dNDVI has proven highly effective in evaluating vegetation damage from wildfires. Areas experiencing severe burn impacts consistently exhibited low dNDVI values, indicating significant vegetation destruction.

This correlation between burn severity and vegetation health metrics fulfills the study's objective to analyze vegetation index changes before and after burning events and provides a quantitative framework for assessing ecological impact.

The temporal analysis of burn severity reveals distinctive patterns throughout the three-month study period from February to April 2024. February established baseline burn patterns with predominantly low severity burns, while March marked a transition period with increased burn severity, and April demonstrated a clear recovery phase. This temporal progression offers valuable insights into the natural cycle of fire disturbance and ecosystem recovery in the region. The research has revealed a significant inverse relationship between burn severity classes and vegetation recovery potential. Lower severity burns (moderate-low and moderate-high) consistently showed higher likelihood of vegetation regrowth, as indicated by both positive dNDVI trends and temporal recovery patterns. Conversely, high severity burns demonstrated minimal recovery signals throughout the observation period, suggesting these intense fires exceed critical ecological thresholds that impede vegetation regeneration. This finding provides empirical evidence addressing the third research objective regarding the relationship between vegetation indices and burn severity levels.

The research identifies distinctive variations in fire impact and recovery patterns across different land use categories. Forest landscapes exhibited the most consistent recovery signals, with regrowth detected across multiple months and severity classes. This suggests inherently higher ecological resilience in forest ecosystems, potentially due to deeper root systems, greater biomass reserves, or evolutionary adaptations to fire disturbance. In contrast, agricultural landscapes demonstrated more limited recovery potential, with regeneration signals appearing later and exclusively within moderate-low severity areas. This temporal delay and restriction to lower severity burns indicates agricultural systems possess more constrained recovery mechanisms and greater vulnerability to fire-induced degradation compared to forested landscapes. These findings highlight the importance of land use context in fire management planning and post-fire restoration efforts.

The research findings have significant implications for wildfire management strategies in Thailand. For moderate-low severity burn areas, the results suggest natural regeneration processes may suffice with minimal intervention, as these areas demonstrated substantial recovery potential within the study timeframe. However, high severity burns area showed persistently limited recovery signals, indicating these zones may require active restoration interventions such as replanting or soil rehabilitation to facilitate ecosystem recovery. The research also identifies critical relationships between burn severity, moisture content, and recurring fire risk. Areas with moderate to light burn severity often retain substantial unconsumed biomass that can serve as fuel for subsequent fires, particularly during drought conditions characterized by elevated temperatures and reduced humidity. This dynamic relationship between vegetation structure, weather conditions, and fire behavior underscores the importance of comprehensive fire management strategies that address both immediate suppression needs and long-term ecological resilience.

6. Future Research and Recommendations

Future research should focus on several key areas to build upon these findings. Firstly, extending the temporal scope of the analysis with longer time series data is crucial for understanding long-term recovery trajectories, especially in high severity burn areas where recovery was limited in this study. Secondly, incorporating additional environmental variables such as climate data, soil properties, and detailed vegetation composition data could provide a more comprehensive understanding of the ecological factors driving differential recovery patterns across various land use types. It is important to acknowledge certain limitations of this study. The limited availability of field data for validation introduces some degree of uncertainty in the results. Therefore, future research should prioritize incorporating ground-truthing efforts to validate and refine the satellite-based assessment. Looking ahead, this research opens up several avenues for future investigation. The application of machine learning and deep learning techniques could further enhance the accuracy and efficiency of burned area detection and vegetation impact assessment. Incorporating high-resolution data sources such as LiDAR or drone imagery could provide more detailed insights into fire behavior and its effects on complex terrain. Long-term impact studies are crucial to fully comprehend the ecological consequences of wildfires, including their effects on biodiversity, soil health, and carbon storage. Such studies would provide invaluable insights into ecosystem recovery mechanisms and inform long-term conservation strategies. Additionally, the development of wildfire occurrence models and real-time warning systems tailored to Thailand's unique ecological and climatic conditions could significantly mitigate fire risks and damages.

Future research should prioritize quantitative analyses of the factors contributing to burns area, including drought severity, vegetation composition, and human activities [57]. Investigating the frequency and severity of fires caused by each factor would provide a more comprehensive understanding of fire risk in these sensitive environments [58].

Acknowledgements

Copernicus Website: We extend our gratitude for providing access to Sentinel-2 satellite imagery through your platform. The high-resolution and extensive coverage of these images have been instrumental in analyzing and monitoring land use changes in the study area, allowing us to gain a deeper understanding of land use dynamics. The Department of Land Development's website provides up-to-date and spatially detailed land use data. This helped to validate and evaluate the satellite-based analysis of land use changes.

References

[1] Talukdar, N. R., Ahmad, F., Goparaju, L., Choudhury, P., Qayum, A. and Rizvi, J., (2024). Forest Fires in Thailand: Spatio-Temporal Distribution and Future Risk Assessment. *Natural Hazards Research*, Vol. 4(1), 87–96. https://doi.org/10.1016/j.nhres.2023.09.002.

[2] Marlier, M. E., DeFries, R. S., Voulgarakis, A., Kinney, P. L., Randerson, J. T., Shindell, D. T., Chen, Y. and Faluvegi, G., (2013). El Niño and Health Risks from Landscape Fire Emissions in Southeast Asia. *Nature Climate Change*, Vol. 3, 131–136. https://doi.org/10.1038/nclimate1658

[3] Tran, B. N., Tanase, M. A., Bennett, L. T. and Aponte, C., (2018). Evaluation of Spectral Indices for Assessing Fire Severity in Australian Temperate Forests. *Remote Sensing*, Vol. 10(11). https://doi.org/10.3390/rs10111680.

[4] Herawati, H. and Santoso, H., (2011). Tropical Forest Susceptibility to and Risk of Fire under Changing Climate: A Review of Fire Nature, Policy, and Institutions in Indonesia. *Forest Policy and Economics*, Vol. 13(4), 227–233. https://doi.org/10.1016/j.forpol.2011.02.006.

[5] Makarabhirom, P., Ganz, D. and Onprom, S., (2001). Community Involvement in Fire Management: Cases and Recommendations for Community-Based Fire Management in Thailand. *Communities in flames*. [Online]. Available: https://gfmc.online/wp-content/uploads/CiF-Ch-2-Thailand.pdf. [Accessed Jul. 23, 2024].

[6] Picos, J., Alonso, L., Bastos, G. and Armesto, J., (2019). Event-Based Integrated Assessment of Environmental Variables and Wildfire Severity through Sentinel-2 Data. *Forests*, Vol. 10(11). https://doi.org/10.3390/f10111021.

[7] Sahdev, S., (2021). Forest Fire Severity Mapping of Humid Tropical Regions: A Geospatial Perspective. *International Journal of Aquatic Science*, Vol. 12(2), 1420-1431.

[8] Delcourt, C., Combee, A., Izbicki, B., Mack, M., Maximov, T., Petrov, R., Rogers, B., Scholten, R., Shestakova, T., van Wees, D. and Veraverbeke, S., (2021). Evaluating the Differenced Normalized Burn Ratio for Assessing Fire Severity Using Sentinel-2 Imagery in Northeast Siberian Larch Forests. *Remote Sensing*, Vol. 13(12). https://doi.org/10.3390/rs13122311.

[9] Ouattara, B., Thiel, M., Sponholz, B., Paeth, H., Yebra, M., Mouillot, F., Kacic, P. and Hackman, K., (2024). Enhancing Burned Area Monitoring with the VIIRS Dataset: A Case Study in Sub-Saharan Africa. *Science of Remote Sensing*, Vol. 10. https://doi.org/10.1016/j.srs.2024.100165.

[10] Ibarra-Bonilla, J. S., Pinedo-Alvarez, A., Jesús A. Prieto-Amparán J. A., Siller-Clavel, P., Santellano-Estrada, E., Alan Álvarez-Holguín. A. and Villarreal-Guerrero, F., (2024). Post-fire Vegetation Dynamics of a Temperate Mixed Forest: An Assessment Based on the Variability of Landsat Spectral Indices. *Trees, Forests and People*, Vol. 17. https://doi.org/10.1016/j.tfp.2024.100648.

[11] Scasta, J. D., Weir, J. R. and Stambaugh, M. C., (2016). Droughts and Wildfires in Western U.S. Rangelands. *Rangelands*, Vol. 38(4), 197-203. https://doi.org/10.1016/j.rala.2016.06.003.

[12] Mahmood, M., and Jumaah, H. (2023). NBR Index-Based Fire Detection Using Sentinel-2 Images and GIS: A Case Study in Mosul Park, Iraq. *International Journal of Geoinformatics*, Vol. 19(3), 67–74. https://doi.org/10.52939/ijg.v19i3.2607.

[13] Da Ponte, E., Alcasena, F., Bhagwat, T., Hu, Z., Eufemia, L., Turetta, A. P. D., Bonatti, M., Sieber, S. and Barr, P. L., (2023). Assessing Wildfire Activity and Forest Loss in Protected Areas of the Amazon Basin. *Applied Geography*, Vol. 157. https://doi.org/10.1016/j.apgeog.2023.102970.

[14] Thirumalai, K., DiNezio, P. N., Okumura, Y. and Deser, C., (2017). The Extreme Temperatures in Southeast Asia are Caused by El Niño and Worsened by Global Warming. *Nature Communications*, Vol. 8(1). https://doi.org/10.1038/ncomms15531.

[15] Avetisyan, D., Velizarova, E. and Filchev, L., (2022). Post-Fire Forest Vegetation State Monitoring Using Satellite Remote Sensing and In-Situ Data. *Remote Sensing*, Vol. 14(24). https://doi.org/10.3390/rs14246266.

[16] Gupta, P., Shukla, A. K. and Shukla, D.P., (2024). Sentinel 2 Based Burn Severity Mapping and Assessment of Post-Fire Impacts on Forests and Buildings in Mizoram, a Northeastern Himalayan Region. *Remote Sensing Applications: Society and Environment*, Vol. 36. https://doi.org/10.1016/j.rsase.2024.101279.

[17] Lee, B. and Howard, F., (2020). Climate Change and Wildfire Risks: A Southeast Asian Perspective. *Environmental Research Journal*, Vol. 21(6), 115-135.

[18] Kala, C. P., (2023). Environmental and Socioeconomic Impacts of Forest Fires: A Call for Multilateral Cooperation and Management Interventions. *Natural Hazards Research*, Vol. 3(2), 286–294. https://doi.org/10.1016/j.nhres.2023.04.003.

[19] Sivrikaya, F., Günlü, A., Küçük, Ö. and Ürker, O., (2024). Forest Fire Risk Mapping Using Landsat 8 OLI Images: Evaluation of the Potential Use of Vegetation Indices. *Ecological Informatics*, Vol. 79. https://doi.org/10.1016/j.ecoinf.2024.102461.

[20] Tran, B. N., Tanase, M. A., Bennett, L. T. and Aponte, C., (2018). Evaluation of Spectral Indices for Assessing Fire Severity in Australian Temperate Forests. *Remote Sensing*, Vol. 10(11). https://doi.org/10.3390/rs10111680.

[21] Fassnacht, F. E., White, J. C., Wulder, M. A. and Næsset, E., (2024). Remote Sensing in Forestry: Current Challenges, Considerations, and Directions. *Forestry: An International Journal of Forest Research*, Vol. 97(1), 11-37. https://doi.org/10.1093/forestry/cpad024.

[22] Sentinel-2 User Handbook. *European Space Agency*. Available: https://sentinels.copernicus.eu/documents/247904/685211/Sentinel-2_User_Handbook. [Accessed Apr. 15, 2024]

[23] Khakhim, N., Kurniawan, A., Wicaksono, P., and Hasrul, A. (2024). Assessment of Empirical Near-Shore Bathymetry Model Using New Emerged PlanetScope Instrument and Sentinel-2 Data in Coastal Shallow Waters. *International Journal of Geoinformatics*, Vol. 20(2), 95–105. https://doi.org/10.52939/ijg.v20i2.3071.

[24] Maslukah, L., Wirasatriya, A., Indrayanti, E., and Krisna, H. (2023). Estimation of Chlorophyll–a and Total Suspended Solid Based on Observation and Sentinel-2 Imagery in Coastal Water Teluk Awur, Jepara-Indonesia. International *Journal of Geoinformatics*, Vol. 19(8), 18–27. https://doi.org/10.52939/ijg.v19i8.2777.

[25] S2 Applications. *European Space Agency*. Available: https://sentiwiki.copernicus.eu/web/s2-applications. [Accessed Oct. 4, 2024].

[26] Khamnoi, W., Homhuan, S., Suwanprasit, C., and Shahnawaz, . (2024). Assessment of Post-Harvest Rice Crop Biomass and Carbon Stock using Remote Sensing Data in Google Earth Engine. *International Journal of Geoinformatics*, Vol. 20(8), 88–101. https://doi.org/10.52939/ijg.v20i8.3459.

[27] Hegazi, E. H., Samak, A. A., Yang, L., Huang, R. and Huang, J., (2023). Prediction of Soil Moisture Content from Sentinel-2 Images Using Convolutional Neural Network (CNN). *Agronomy*, Vol. 13(3). https://doi.org/10.3390/agronomy13030656.

[28] Farhadi, H., Ebadi, H. and Kiani, A., (2023). BADI: A Novel Burned Area Detection Index for Sentinel-2 Imagery Using Google Earth Engine Platform. *ISPRS Annals of the Photogrammetry, Remote Sensing and Spatial Information Sciences, Vol. X-4/W1-2022, GeoSpatial Conference 2022 – Joint 6th SMPR and 4th GIResearch Conferences, 19–22 February 2023*, Tehran, Iran (virtual). https://doi.org/10.5194/isprs-annals-X-4-W1-2022-179-2023.

[29] Pinto, M. M., Trigo, R. M., Trigo, I. F. and DaCamara, C. C., (2021). Practical Method for High-Resolution Burned Area Monitoring Using Sentinel-2 and VIIRS. *Remote Sensing*, Vol. 13(9). https://doi.org/10.3390/rs13091608.

[30] Salvoldi, M., Siaki, G., Sprintsin, M. and Karnieli, A., (2020). Burned Area Mapping Using Multi-Temporal Sentinel-2 Data by Applying the Relative Differenced Aerosol-Free Vegetation Index (RdAFRI). *Remote Sensing*, Vol. 12(17). https://doi.org/10.3390/rs12172753.

[31] Sali, M., Piaser, E., Boschetti, M., Brivio, P. A., Sona, G., Bordogna, G. and Stroppiana, D., (2021). A Burned Area Mapping Algorithm for Sentinel-2 Data Based on Approximate Reasoning and Region Growing. *Remote Sensing*, Vol. 13(11). https://doi.org/10.3390/rs13112214.

[32] Roteta, E., Bastarrika, A., Padilla, M., Storm, T. and Chuvieco, E., (2019). Development of a Sentinel-2 Burned Area Algorithm: Generation of a Small Fire Database for Sub-Saharan Africa. *Remote Sensing of Environment*, Vol. 222, 1-17. https://doi.org/10.1016/j.rse.2018.12.011.

[33] Roy, D. P., Boschetti, L. and Trigg, S. N., (2006). Remote Sensing of Fire Severity: Assessing the Performance of the Normalized Burn Ratio. *IEEE Geoscience and Remote Sensing Letter*s, Vol. 3(1), 112–116. https://doi.org/10.1109/LGRS.2005.858485.

[34] Gao, B. C., (1996). NDWI-A Normalized Difference Water Index for Remote Sensing of Vegetation Liquid Water from Space. *Remote Sensing of Environment*, Vol. 58(3), 257-266. https://doi.org/10.1016/S0034-4257(96)00067-3.

[35] Parks, S. A., Dillon, G. K. and Miller, C., (2014). A New Metric for Quantifying Burn Severity: The Relativized Burn Ratio. *Remote Sensing*, Vol. 6(3), 1827-1844. https://doi.org/10.3390/rs6031827.

[36] Lutes, D. C., Keane, R. E., Caratti, J. F., Key, C. H., Benson, N. C., Sutherland, S. and Gangi, L. J., (2006). *FIREMON: Fire Effects Monitoring and Inventory System*. General Technical Report RMRS-GTR-164-CD, Rocky Mountain Research Station, USDA Forest Service, Fort Collins.

[37] De Simone, W., Di Musciano, M., Di Cecco, V., Ferella, G. and Frattaroli, A. R., (2020). The Potentiality of Sentinel-2 to Assess the Effect of Fire Events on Mediterranean Mountain Vegetation. *Plant Sociology*, Vol. 57(1), 11-22. https://doi.org/10.3897/pls2020571/02.

[38] Southern Research Station, USDA Forest Service., (2008). *Forest Science in the South-2008*. Science Update SRS-016, Asheville, NC: U.S. Department of Agriculture.

[39] Fitzpatrick-Lins, K., (1981). Comparison of Sampling Procedures and Data Analysis for Land Use and Land Cover Maps. *Photogrammetric Engineering and Remote Sensing*, Vol. 47(3), 343-351.

[40] Gates, D. M., Keegan, H. J., Schleter, J. C. and Weidner, V. R., (1965). Spectral Properties of Plants. *Applied Optics*, Vol. 4(1), 11-20. https://doi.org/10.1364/AO.4.000011.

[41] Piloyan, A. (2023). Assessing Spatio-temporal Changes of Floating Aquatic Vegetation in Lake Sevan Using Landsat Imagery and Vegetation Indices. *International Journal of Geoinformatics*, Vol. 19(11), 1–11. https://doi.org/ 10.52939/ijg.v19i11.2913.

[42] Tucker, C. J., (1979). Red and Photographic Infrared Linear Combinations for Monitoring Vegetation. *Remote Sensing of Environment*, Vol. 8(2), 127-150. https://doi.org/10.1016/0034-4257(79)90013-0.

[43] Xu, H., (2006). Modification of Normalised Difference Water Index (NDWI) to Enhance Open Water Features in Remotely Sensed Imagery. *International Journal of Remote Sensing*, Vol. 27(14), 3025-3033. https://doi.org/10.1080/01431160600589179.

[44] Chen, X., Vogelmann, J.E., Rollins, M., Ohlen, D., Key, C.H., Yang, L., Huang, C. and Shi, H., (2011). Detecting Post-Fire Burn Severity and Vegetation Recovery Using Multitemporal Remote Sensing Spectral Indices and Field-Collected Composite Burn Index Data in a Ponderosa Pine Forest. *International Journal of Remote Sensing*, Vol. 32(23), 7905–7927. https://doi.org/10.1080/01431161.2010.524678

[45] Rakholia, S., Mehta, A. and Suthar, B., (2021). Forest Fire Monitoring of Shoolpaneshwar Wildlife Sanctuary, Gujarat, India Using Geospatial Techniques. *Current Science*, Vol. 119(12), 1974-1981. https://doi.org/10.18520/cs/v119/i12/1974-1981.

[46] McKenna, P., Phinn, S. and Erskine, P. D., (2018). Fire Severity and Vegetation Recovery on Mine Site Rehabilitation Using WorldView-3 Imagery. *Fire*, Vol. 1(2). https://doi.org/10.3390/fire1020022.

[47] Khamchiangta, D. and Dhakal, S., (2020). Time Series Analysis of Land Use and Land Cover Changes related to Urban Heat Island Intensity: Case of the Bangkok Metropolitan Area in Thailand. *Journal of Urban Management*, Vol. 9, 383-395. https://doi.org/10.1016/j.jum.2020.09.001.

[48] Van Wagtendonk, J. W., (1996). Use of a Deterministic Fire Growth Model to Test Fuel Treatments, *University of California, Centers for Water and Wildland Resources*, 1155–1165.

[49] Keeley, J. E., (2009). Fire Intensity, Fire Severity and Burn Severity: A Brief Review and Suggested Usage. *International Journal of Wildland Fire*, Vol. 18, 116-126. https://doi.org/10.1071/WF07049.

[50] Waldrop, T. A., Hagan, D. L. and Simon, D. M., (2016). Repeated Application of Fuel Reduction Treatments in the Southern Appalachian Mountains, USA: Implications for Achieving Management Goals. *Fire Ecology*, Vol. 12, 28-47. https://doi.org/10.4996/fireecology.1202028.

[51] Moreno, J. M., Morales-Molino, C., Torres, I. and Arianoutsou, M., (2021). Fire in Mediterranean Pine Forests: Past, Present and Future. *Springer, Cham*, Vol. 38, 421-456. https://doi.org/10.1007/978-3-030-63625-8_21.

[52] Parks, S. A., Dillon, G. K. and Miller, C., (2014). A New Metric for Quantifying Burn Severity: The Relativized Burn Ratio. *Remote Sensing*, Vol. 6(3), 1827-1844. https://doi.org/10.3390/rs6031827.

[53] Morgan, P., Keane, R. E., Dillon, G. K., Jain, T. B., Hudak, A. T., Karau, E. C., Sikkink, P., Holden, Z. A. and Strand, E. K., (2014). Challenges of Assessing Fire and Burn Severity using Field Measures, Remote Sensing and Modelling. *International Journal of Wildland Fire*, Vol. 23(8), 1045-1060. https://doi.org/10.1071/WF13058.

[54] Marcos, B., Gonçalves, J., Alcaraz-Segura, D., Cunha M. and Honrado, J. P., (2023). Assessing the Resilience of Ecosystem Functioning to Wildfires using Satellite-Derived Metrics of Post-Fire Trajectories. *Remote Sensing of Environment*, Vol. 286. https://doi.org/10.1016/j.rse.2022.113441.

[55] Amiro, B. D., Orchansky, A. L., Barr, A., Black, A., Chambers, S., Chapin III, F S., Goulden, M., Litvak, M., Liu, H. P., McCaughey, H., Mcmillan, A. and Randerson, J., (2006). The Effect of Post-Fire Stand Age on the Boreal Forest Energy Balance. *Agricultural and Forest Meteorology*, Vol. 140(1-4), 41-50. https://doi.org/10.1016/j.agrformet.2006.02.014.

[56] Keeley, J., (2009). Fire Intensity, Fire Severity and Burn Severity: A Brief Review and Suggested Usage. *International Journal of Wildland Fire*, Vol.18, 116-126. https://doi.org/10.1071/WF07049.

[57] Ge, W., Li, X., Xie, M. and Yu, B., (2023). Quantitative Evaluation of Drought Risk Related to Vegetation Productivity in China. *Journal of Hydrology*, Vol. 623(6). https://doi.org/10.1016/j.jhydrol.2023.129877.

[58] Osborne, T. Z., Kobziar, L. N. and Inglett, P. W., (2013). Fire and Water: New Perspectives on Fire's Role in Shaping Wetland Ecosystems. *Fire Ecology*, Vol. 9, 1-5. https://doi.org/10.4996/fireecology.0901001.